A QUANTUM-CHEMICAL STUDY OF POLAR $SrTiO_3$ (110) SURFACE AND OXYGEN-VACANCY DEFECTS THEREIN

Arvids STASHANS and Sheyla SERRANO

Centro de Investigación en Física de la Materia Condensada, Corporación de Física Fundamental y Aplicada, Apartado 17-12-637, Quito, Ecuador

Surfaces of strontium titanate are of immense technological importance due to their catalytic properties and a wide range of applications. Using an advanced quantum-chemical semi-empirical method developed for crystal studies we investigate the polar $SrTiO_3$ (110) surface. Oxygen vacancies and F centers (two electrons trapped at an oxygen vacancy) are included in our computations in order to obtain basic information on the structural and electronic properties due to the presence of these point defects. Our studies are carried out for both crystallographic lattices, cubic and tetragonal. The comparison between our results and the available experimental data is presented in the manuscript.

Keywords: $SrTiO_3$, (110) polar surface, quantum-chemistry, point defects

1. Introduction

Surfaces of the perovskite-type crystals are of great scientific interest and are also important due to their technological applications. $SrTiO_3$ has attracted a special attention and is generally regarded as a model substance of the perovskite group. A number of studies have been done for different surfaces of the $SrTiO_3$ crystal [1, 2]. These investigations have been carried out for both, the stoichiometric surfaces [3-5] and the surfaces containing different defects [6, 7]. Surfaces of the $SrTiO_3$ crystal may give rise to a possible ferroelectric reconstruction [8] and may become metallic on introduction oxygen vacancies [9]. Nowadays, surfaces of the $SrTiO_3$ crystals have become of the technological use due to their catalytic properties [1] and are also widely used as epitaxial growth substrates for the high temperature superconductor (HTSC) thin films [10] as well as in the high T_C-based heterostructures [11].

It is well recognized that the surface defects such as oxygen vacancies play an important role as a reaction centers in the catalytic processes [12, 13]. Therefore, in order to improve the quality of HTSC thin films, it is necessary and important to study the effect of surface oxygen vacancies on the electronic and structural properties of the $SrTiO_3$ crystal. In contrast to the (100) surfaces, basic properties of the $SrTiO_3$ (110) surface have not been sufficiently studied up to date, though this surface is a popular substrate for epitaxial growth of the so-called a-axis oriented HTSC films. These films compose junction devices in which superconducting tunneling is expected to take place in parallel to the two-dimensional CuO_2 planes. Thus it is important to investigate changes in microscopic structure and electronic properties of the $SrTiO_3$ (110) surface due to the presence of oxygen-vacancy defects. Up to now this surface has been studied

mainly experimentally by ultraviolet photoemission spectroscopy, X-ray photoemission spectroscopy and low energy electron diffraction techniques [14]. Recent scanning tunneling microscopy and spectroscopy observations [15] have revealed in-gap states, which could imply the presence of the so-called F-type centers on the $SrTiO_3$ surfaces.

In this paper, the electronic structure of the $SrTiO_3$ (110) surface containing oxygen-vacancy defects as well as the electronic structure of a pure surface is investigated by means of the advanced quantum-chemical method developed for crystals. Geometry optimization is performed to obtain the lattice relaxation around the point defects and equilibrium configurations of the defective surfaces.

2. Method of calculation

The employed method of periodically repeated large unit cells (LUCs) [16] is designed for the calculation of the total energy and electronic structure of crystals. We preferred to use the LUC model because of its advantage compared to different cluster models, for example, a better treatment of the exchange interaction. A full discussion of the computational relations for calculating the total energy of the crystal within the framework of the LUC approach is given in Refs. 16-18. In the present work we shall only outline the basic ideas of the method.

In the LUC $\boldsymbol{k} = 0$ approximation, the Fock matrix elements are made self-consistent through the density matrix elements obtained in the following manner:

$$\mathrm{P}^{\boldsymbol{0}}_{\boldsymbol{pq}} = \frac{1}{\mathrm{N}} \sum_{k} \mathrm{P}_{\boldsymbol{pq}}(\boldsymbol{k}) \exp(\mathrm{i}\boldsymbol{k}\boldsymbol{R}_{v}) \qquad (1)$$

Here the summation is carried out over all **k** values in the reduced Brillouin zone (BZ)

of the LUC. In this way the information regarding the density matrix $P_{pq}(\mathbf{k})$ is obtained only in the point **k**=0. However, it has been proven [16, 19] that the computation of the electronic structure of the unit cell at $\boldsymbol{k} = 0$ in the reduced BZ is equivalent to a band structure calculation at those BZ $\boldsymbol{k}$ points, which transform to the reduced BZ center on extending the unit cell. As indicated by numerous studies [20-22], eight-fold or even four-fold-symmetric extension of the primitive unit cell proves to be completely sufficient to reproduce correctly the electronic band structure of a given crystal.

Our method is based on a semi-empirical modification of the molecular orbital (MO) theory with a specific parametrization scheme [23]. Some atomic parameters are used to reproduce main features of a given crystal and to reduce considerably the computational time. Thus our method is not cumbersome and is applicable to extended systems with a complex structure and a mixed chemical bonding. The $SrTiO_3$ crystal has been parametrized by us before [24] where also details of the bulk crystal computations are given. The numerical values of atomic parameters are shown in table 1. We would like to note that our method has been used before successfully to calculate surfaces. Some examples include study of charge and potential distribution near the GaP (110) surface [25], OH^- adsorption on the perfect rutile (TiO_2) (001) surface [26], and also calculation of organic adsorbates on the rutile (110) surface [27, 28].

Our method already has been applied to study the $SrTiO_3$ crystal giving encouraging results. The examples include study of La-doping [24, 29], calculation of oxygen vacancies and F centers in crystal bulk [30] as well as determination of the self-trapped and impurity-trapped hole polarons [31] in this material.

3. Results and discussion

3.1. A pure $SrTiO_3$ (110) surface

We have chosen to use the periodic LUC model within the Hartree-Fock theory due to its availability for extended systems, reliability in point defect studies and high accuracy of the method in determination of the equilibrium configurations for both ground and excited states of a system. The method as it is implemented into the CLUSTERD computer code [17] uses a number of semi-empirical parameters, which allows one to reproduce with sufficiently high precision structural and band structure properties of a given crystal. As demonstrated by numerous computations [16, 24, 32-34], an eight-fold or even four-fold-symmetric extension of the primitive unit cell proves to be completely sufficient to reproduce correctly the electronic density distribution of the crystal bulk and/or surface. Hence we have chosen to exploit 80-atomic LUC, which corresponds to the 16-fold extension of the primitive 5-atomic unit cell. This supercell is used for both a pure and defective surface calculations. The large size of the LUC was chosen to eliminate any possible mutual defect-defect interactions, i.e., to allow study of a *single point defect* within the periodic model. The surface was modeled as a single slab consisting of eight layers and applying 2D periodicity in the <001> and $<\bar{1}10>$ directions. The translation vectors in the direction <110> were defined to be equal to zero. The bulk lattice parameters, a = 3.90 Å for the cubic structure and a = 3.88 Å, c = 3.92 Å for the tetragonal structure, fitted by us before [24, 31] were used.

The $SrTiO_3$ (110) surface is a polar one. This means that it consists of periodically repeated positively and negatively charged atomic layers (Fig. 1). The negatively charged layers contain only oxygens while the positively charged layers

consist of oxygen, titanium and strontium atoms. In order to characterize the perfect $SrTiO_3$ (110) surface, the equilibrium geometry was calculated allowing relaxing all atoms in the two surface-topmost layers from both sides of the slab. We considered different relaxation modes in both, the direction perpendicular to the surface and within the surface plain. An automated geometry optimization was also performed using the downhill simplex method in multidimensions [35]. As a result it was found that atomic movements within the plains parallel to the surface are negligible while their relaxation in the direction perpendicular to the surface is considerable. As it is shown in Fig. 2 for the cubic lattice, the strontium layer in the left-hand side moves inward by 0.36 Å and the nearest oxygen layer moves outward by 0.16 Å. These displacements can be understood taking into account the polar character of the surface and thus the importance of the Coulomb electrostatic interaction. The two above-mentioned layers have opposite electrical charge and thus experience mutual attraction. That is why they move towards each other. In the slab's right-hand side we observe that the oxygen layer moves inward the crystal by 0.07 Å while for the topmost layer we find the following pattern of atomic displacements. The titaniums of this layer move inward by around 0.20 Å while the oxygens of the same layer find themselves displaced outward the crystal's bulk by approximately 0.07 Å. Again, the Coulomb electrostatic interaction plays very important role in these movements. The inward titanium movements and the outward oxygen movements are due to the attractive and repulsive interactions, respectively, with the next atomic layer, which is charged negatively because consists only of oxygens. In general, we have to note that the observed atomic rearrangement due to the surface creation is considerably larger as calculated before by one of us for the TiO_2 (110) surface [32] and the $SrTiO_3$ (001) surface [36]. In those studies the same

computer code and physical model was used. In our mind, the obtained larger atomic displacements are due to the fact that the $SrTiO_3$ (110) surface is a polar one. These results also support the idea that the observed drastic modification of the surface can not be related only to the formation of point defects but have to be interpreted in terms of the formation of the so-called non-perovskite phases [37-39].

The atomic relaxation was performed for both cubic and tetragonal structures of the $SrTiO_3$ crystal. We did not find, however, noticeable differences in the surface reconstruction for these two crystallographic structures. A bit smaller, around 0.02 Å, atomic movements for the tetragonal lattice were observed. The calculated relaxation energies as a difference between the total energies for the fully relaxed and unrelaxed systems, were found to be equal to 10.3 eV and 9.3 eV for the cubic and tetragonal lattices, respectively. The tetragonal structure of the crystal exists at lower temperatures and thus it is more stable. Therefore, one finds slightly smaller atomic displacements and relaxation energy for this crystallographic lattice. In addition, as it will be discussed below, the chemical bonding for the tetragonal structure of the crystal is more covalent making atomic movements more restricted. Thus optimized geometry was used later for the electronic structure calculations.

We have calculated density of states (DOS) for both crystalline structures (see Figs. 3 and 4). The lower valence band (LVB) is composed mainly of the O 2s states while the upper valence band (UVB) predominantly is O 2p in nature. The narrow sub-band of the Sr 4p states is located just between two valence bands. The bottom of the conduction band (CB) is composed mainly of the Ti 3d states with some admixture of the Sr 5s states. We have to note that for both crystallographic phases there is a noticeable admixture of the Ti 3d states in the UVB. We did not find any local states

within the gap between the UVB and the CB in the case of pure surfaces. Obviously, these in-gap electronic states are related to the surface oxygen vacancies and/or F centers in accordance with another studies [15, 40]. The calculated effective charges on atoms using the Löwdin population analysis [41] were found to be different depending on their position. For the cubic structure, the maximal effective charges were obtained in the center of the slab, q(Ti) = +2.15 ***e***, q(Sr) = +1.87 ***e*** and q(O) = -1.36 ***e***, the minimal effective charges were found on atoms situated on the slab's periphery, q(Ti) = +1.85 ***e***, q(Sr) = +1.68 ***e*** and q(O) = -1.08 ***e***. The calculated effective charges on atoms for the tetragonal structure exhibit the same behavior. The maximal effective charges are in the center of the slab, q(Ti) = +1.95 ***e***, q(Sr) = +1.87 ***e*** and q(O) = -1.25 ***e***, while the minimal effective charges are on the outer atoms, q(Ti) = +1.75 ***e***, q(Sr) = +1.68 ***e*** and q(O) = -1.02 ***e***. As one can notice we have obtained less negative charges on oxygens and less positive charges on titaniums for the tetragonal structure. This effect points to the fact that the tetragonal lattice has higher degree of covalency. This can be also seen from the composition of the UVB (Figs. 3 and 4), which points out the larger admixture of the Ti 3d AOs in the UVB in the case of the tetragonal phase.

3.2. Oxygen-vacancy and its properties

In order to study oxygen vacancies on the $SrTiO_3$ (110) surface and their influence upon different material properties, we made use of 80-atomic LUC taking out one oxygen ion, i.e., creating a vacancy, V_0. The charge of the V_0 with respect to the perfect crystalline lattice is +2, i.e., we deal with the so-called charged point defect within the periodic model. The problem for net charge has been discussed in detail in

Ref. 42, in which the reliability of the charged periodic model has been shown. According to [42] the Coulomb energy E^c of a periodic array is written as follows:

$$E^c = \frac{1}{2}\sum_{ij}\frac{q_i q_j}{\left|\mathbf{r}_{j1}-\mathbf{r}_{i0}\right|}\mathrm{erf}(\gamma^{1/2}\left|\mathbf{r}_{j1}-\mathbf{r}_{i0}\right|) + \frac{2\pi}{v_0}\sum_{\mathbf{G}\neq 0}\frac{1}{\mathbf{G}^2}\left|S(\mathbf{G})\right|^2 \exp(-\mathbf{G}^2/4\gamma) - \left(\frac{\gamma}{\pi}\right)^{1/2}\sum_i q_i^2 - \frac{\pi Q^2}{2v_0\gamma} \quad (2)$$

where the term $j = i$ is omitted if 1=0, q_I is the charge on ion i, γ is the Ewald parameter, v_0 is the volume of the repeating 80-atomic LUC, the **G** is the reciprocal-lattice vector of the superlattice, the S(**G**) is the structure factor of the repeating unit, and Q is the net charge of the unit, which is equal to +2 in our case. The last term of equation (2) appearing due to the net charge Q does not depend on the positions of the ions within the LUC. In the present work we compare the total energies of different spatial configurations *within the same* type of defect, i.e., within *the constant* last term of equation (2), as a result it is not necessary to take into account the effect of the last term.

The strontium titanate is known to exist in two crystallographic phases, cubic and tetragonal, so both phases were considered in the calculations. As it is shown in Fig. 5, the V_0 finds itself surrounded by all three types of atoms. In order to obtain the energy-minimum configuration, we allowed 19 defect-closest atoms to move freely from their initial lattice sites. The automated geometry optimization procedure [35] was exploited to reach the equilibrium configuration of the system. The summary of the atomic displacements is given in table 2. As one can see the atomic movements were found not to exceed 0.06 Å and 0.05 Å for the cubic and tetragonal phases, respectively. Magnitude of the atomic movements was found to be of the same order as for the V_0 studies on the $SrTiO_3$ (001) non-polar surface [36]. The atomic relaxation, in general,

obeys the Coulomb electrostatic interaction law. The positively charged Ti and Sr atoms move outward the positively charged V_0, while the negatively charged O atoms move toward the V_0. The calculated relaxation energy, E_{rel}, as a difference between the relaxed and unrelaxed crystal states containing V_0 was found to be equal to 9.67 eV and 7.62 eV for the cubic and tetragonal phases, respectively. Although the magnitude of relaxation is not very large we obtain considerable values for the relaxation energies. This might be explained by a noticeable electronic density redistribution in the defective region due to the V_0 presence. The fact that the E_{rel} is larger for the cubic phase might be explained by slightly larger atomic displacements in this phase and also due to the more rigid crystalline lattice in the tetragonal phase existing at lower temperatures.

It is worth to compare our results of atomic displacements around the V_0 center with similar studies of these defects on the (100) MgO surface [43] and crystal bulk [44]. In all cases outward displacements for positively charged atoms and inward movements for negatively charged atoms with respect to the oxygen vacancy are obtained. However, in the case of more ionic MgO crystal the atomic relaxation is larger in magnitude, i.e. up to 11% of the initial inter-atomic distance, comparing to our case. This implies one more time the importance of the covalent contribution into the chemical bonding of the $SrTiO_3$ crystal. Due to the larger degree of the covalency compared to the ionic MgO crystal the atoms are less “mobile” in the $SrTiO_3$ crystal leading to the smaller atomic displacements.

Table 3 displays charges on atoms situated in the defective region. As one can see there exist electronic density redistribution due to the V_0 creation. A short analysis points to the following general tendency in the charge redistribution. The V_0-surrounding negative O atoms become a bit less negative and the defective-closest Ti

atoms become a bit less positive. This implies that the V_0 changes slightly the nature of the chemical bonding between the atoms situated in the defective region making it more covalent especially between the Ti and O atoms.

3.3. F center and its properties

Two electrons were added to the system containing V_0 to study F centers and their influence upon the structural and electronic properties of this material. Similarly as for the V_0, we computed this point defect for both crystallographic lattices of the $SrTiO_3$ crystal. The summarized results of atomic displacements around the F center are given in table 2 and Fig. 5. showing the following pattern. The directions of atomic movements, in general, remain the same but their magnitudes diminish. This is anticipated because instead of the positively charged V_0 point defect we have "neutral" F center. The obtained relaxation energies are also considerably smaller compared to the case of the V_0 defects. The obtained values of E_{rel} are equal to 4.26 eV and 2.50 eV for cubic and tetragonal structures, respectively.

Analysis of charges on atoms situated around the F center shows a considerable density redistribution for the two Sr atoms, Sr(1) and Sr(13). These two atoms situated along the <101> and <10$\bar{1}$> directions with respect to the F center are the two defect-closest atoms, which implies that the F center is well localized within the O vacancy region similarly as it was found for MgO [43] and α-Al_2O_3 [45, 46] crystals. However, our result of the electron density redistribution on the closest Sr atoms is somewhat different from the similar studies carried out for the $SrTiO_3$ (001) surface [36], where the wave function of the two extra electrons was found on the defect-closest Ti atoms.

The important feature of a material is the occurrence of electronic states within the band-gap region due to the F centers. As it was established before for the $SrTiO_3$ (100) surface, the in-gap electronic states are ascribed to the Ti 3d – O vacancy complexes [47, 48]. This was also confirmed in our previous calculations [36] for this type of surface. However, in the case of the $SrTiO_3$ (110) surface, we find an electronic state in the middle of the energy gap composed mainly of the Sr states of the two defect-closest Sr atoms. This is true for both, cubic and tetragonal structures. In our mind, this occurs due to the different surface morphology and the fact that for the (110) surface Ti atoms turn to be considerably less positive compared to the (001) surface case [36]. This unexpected result is in an agreement with the scanning microscopy and spectroscopy data [15] as well as the theoretical analysis of charge transfer phenomenon [14] in the $SrTiO_3$ crystal.

4. Conclusions

We have presented the computational study of oxygen vacancies and F centers on the $SrTiO_3$ (110) surfaces as well as the investigation of the same pure surface. The structural and electronic properties are studied within the same computational method and applying the same physical model to describe the surface. The study of the perfect (110) surface reveals the importance of the Coulomb interaction between atoms, which leads to very large atomic displacements for the surface layers. These results also support the idea that the observed drastic modification of the surface can not be related only to the formation of point defects but have to be interpreted in terms of the formation of non-perovskite phases [37-39].

The obtained results of structure relaxation around the oxygen vacancies and F centers point to the significant role of the Coulomb interaction in this semi-ionic material. However, in the case of the oxygen vacancies the analysis of the electronic density redistribution leads to the conclusion that these defects make material more covalent due to the stronger hybridization between the O 2p and Ti 3d states. Wave functions of the F centers are found on the two defect-closest Sr atoms pointing to localization of two electrons within the O vacancy region. As a result we also find an electronic state in the middle of the energy gap composed mainly of the Sr 5s states.

Acknowledgments

The authors are grateful to Paul Sánchez for preparation of Figs. 3 and 4.

References

[1] V. E. Henrich and P. A. Cox, The Surface Science of Metal Oxides (Cambridge University Press, Cambridge, 1994).

[2] C. Noguera, Physics and Chemistry at Oxide Surfaces (Cambridge University Press, Cambridge, 1995).

[3] F. M. F. de Groot, J. Faber, J. J. Michiels, M. T. Czyzyk, M. Abbate, and J. C. Fuggle, Phys. Rev. B 48 (1993) 2074.

[4] O. V. Krasovska, E. E. Krasovskii, and V. N. Antonov, Solid State Commun. 97 (1996) 1019.

[5] H. Haruyama, S. Kodeira, Y. Aiura, H. Bando, Y. Nishihara, T. Maruyama, Y. Sakisaka, and H. Kato, Phys. Rev, B 53 (1996) 8032.

[6] V. E. Henrich, Prog. Surf. Sci. 14 (1983) 175.

[7] R. Courths, J. Noffke, H. Wern, and R. Heise, Phys. Rev. B 42 (1990) 9127.

[8] V. Ravikumar, D. Wolf, and V. P. David, Phys. Rev. Lett. 74 (1995) 960.

[9] S. Kimura, J. Yamauchi, M. Tsukada, and S. Watanabe, Phys. Rev. B 51 (1995) 11049.

[10] V. C. Matijasevic, B. Ilge, B. Stäuble-Pümpin, G. Rietveld, F. Tuinstra, and J. E. Moorij, Phys. Rev. Lett. 76 (1996) 4765.

[11] Yu. A. Boikov and T. Claeson, J. Appl. Phys. 81 (1997) 3232.

[12] S. Ferrer and G. A. Somorjai, Surf. Sci. 94 (1980) 41.

[13] C. A. Muryn, P. J. Hardman, J. J. Crouch, G. N. Raiker, G. Thornton and D. S.-L. Law, Surf. Sci. 251/252 (1991) 747.

[14] Y. Aiura, H. Bando, Y. Nishihara, Y. Haruyama, S. Kodaira, T. Komeda, Y. Sakisaka, T. Maruyama, and H. Kato, Advances in Superconductivity (Springer,

Tokyo, 1994), Vol. 6, p. 983.

[15] H. Bando, Y. Aiura, Y. Haruyama, T. Shimizu, and Y. Nishihara, J. Vac. Sci. Technol. B 13 (1995) 1150.

[16] A. Shluger and E. Stefanovich, Phys. Rev. B 42 (1990) 9664.

[17] E. V. Stefanovich, E. K. Shidlovskaya, A. L. Shluger, and M. A. Zakharov, Phys. Status Solidi B 160 (1990) 529.

[18] P. V. Smith, J. E. Szymanski, and J. A. D. Matthews, J. Phys. C 18 (1985) 3157.

[19] R. A. Evarestov, Quantum-Chemical Methods of Solid State Theory (Leningrad State University Press, Leningrad, 1982).

[20] Yu. F. Zhukovskii, E. A. Kotomin, R. M. Nieminen, and A. Stashans, Comput. Mater. Sci. 7 (1997) 285.

[21] A. Stashans and M. Kitamura, Solid State Commun. 99 (1996) 583.

[22] F. Erazo and A. Stashans, Phil. Mag. B 80 (2000) 1499.

[23] A. Shluger, Theor. Chim. Acta 66 (1985) 355.

[24] A. Stashans and P. Sánchez, Mater. Lett. 44 (2000) 153.

[25] E. V. Stefanovich and A. L. Shluger, J. Phys.: Condens. Matter 6 (1994) 4255.

[26] A. Stashans, S. Lunell, and R. W. Grimes, J. Phys. Chem. Solids 57 (1996) 1293.

[27] P. Persson, A. Stashans, R. Bergström, and S. Lunell, Int. J. Quant. Chem. 70 (1998) 1055.

[28] L. Patthey, H. Rensmo, P. Persson, K. Westermark, L. Vayssieres, A. Stashans, Å. Petersson, P. Brühwiler, H. Siegbahn, S. Lunell, and N. Mårtensson, J. Chem. Phys. 110 (1999) 5913.

[29] H. Pinto, A. Stashans, and P. Sánchez, Defects and Surface-Induced Effects in Advanced Perovskites, NATO Science Series, Vol. 77, p. 67 (Kluwer Academic

Publishers, Dordrecht, 2000).

[30] A. Stashans and F. Vargas, Mater. Lett. 50 (2001) 145.

[31] A. Stashans, Mater. Chem. Phys. 68 (2001) 124.

[32] A. Stashans, S. Lunell, R. Bergström, A. Hagfeldt, and S.-E. Lindquist, Phys. Rev. B 53 (1996) 159.

[33] A. Stashans and M. Kitamura, J. Phys. Chem. Solids 58 (1997) 777.

[34] S. Lunell, A. Stashans, L. Ojamäe, H. Lindström, and A. Hagfeldt, J. Am. Chem. Soc. 119 (1997) 7334.

[35] W. H. Press, B. P. Flannery, S. A. Teukolsky, and T. Vetterling, Numerical Recipes: The Art of Scientific Computing (Cambridge University Press, New York, 1986).

[36] A. Stashans, F. Erazo, J. Ortiz, and P. Valverde, Phil. Mag. B (2001), in press.

[37] Y. Liang and D. A. Bonnell, Surf. Sci. 310 (1994) 128.

[38] Y. Liang and D. A. Bonnell, J. Am. Ceram. Soc. 78 (1995) 2633.

[39] K. Szot and W. Speier, Phys. Rev. B 60 (1999) 5909.

[40] Y. Aiura, H. Bando, T. Maruyama, Y. Nishihara, Y. Haruyama, S. Kodaira, T. Komeda, Y. Sakisaka, and H. Kato, Physica C 235-240 (1994) 1009.

[41] P.-O. Löwdin, J. Chem. Phys. 18 (1950) 365.

[42] M. Leslie and M. J. Gillan, J. Phys. C 18 (1985) 973.

[43] A. M. Ferrari and G. Pacchioni, J. Phys. Chem. 99 (1995) 17010.

[44] R. Pandey and J. M. Vail, J. Phys.: Condens. Matter 1 (1989) 2801.

[45] A. Stashans, E. Kotomin, and J.-L. Calais, Phys. Rev. B 49 (1994) 14854.

[46] A. Stashans, J.-L. Calais, and E. Kotomin, Proc. Europ. Conf. Comput. Chem (AIP Press, New York, 1995), p. 177.

[47] V. E. Henrich, G. Dresselhaus, and H. J. Zeiger, Phys. Rev. B 17 (1978) 4908.

[48] B. Cord and R. Courths, Surf. Sci. 162 (1985) 34.

Table 1

(a) Atomic parameters used in the present work.

Atom	AO	ζ	E_{neg}	P^0	β
Sr	5s	1.59	11.15	0.18	-0.4
	4p	2.80	37.5	2.00	-4.5
Ti	4s	1.4	3.7	0.65	-0.5
	4p	1.1	-15.0	0.04	-0.5
	3d	1.93	7.2	0.55	-9.0
O	2s	2.27	4.5	1.974	-16.0
	2p	1.86	-12.6	1.96	-16.0
La	6s	1.0	11.3	0.40	-0.4
	6p	1.0	2.0	0.01	-0.4
	5d	1.97	11.0	0.08	-6.3

(b) Two-center parameters $\alpha_{\mu B}$ (au^{-1}), the numbers in the parenthesis show the corresponding parameter for the tetragonal phase.

A	B			
	Sr	Ti	O	La
Sr	0.15	0.55	0.25	0.00
Ti	0.09 (0.10)	0.13 (0.16)	0.10 (0.14)	0.00
O	0.59	0.38 (0.362)	0.15	0.53
La	0.01	0.02	0.03	0.01

Table 2

Atomic displacements (in Å) in the defective region containing either V_0 or F center.

The atomic numeration corresponds to the one given in Fig. 5.

ATOM	CUBIC STRUCTURE		TETRAGONAL STRUCTURE	
	V_0	F center	V_0	F center
Sr (1)	0.05	0.03	0.04	0.04
O (2)	0.04	0.02	0.02	0.02
O (3)	0.04	0.03	0.05	0.03
O (4)	0.06	0.04	0.05	0.04
Ti (5)	0.05	0.03	0.03	0.03
Ti (6)	0.06	0.04	0.05	0.04
O (7)	0.04	0.03	0.04	0.03
O (8)	0.04	0.02	0.03	0.03
O (9)	0.06	0.04	0.04	0.04
Sr (10)	0.04	0.02	0.03	0.03
O (11)	0.02	0.01	0.01	0.01
O (12)	0.05	0.03	0.02	0.02
Sr (13)	0.04	0.03	0.04	0.03
Sr (14)	0.03	0.02	0.03	0.03
O (15)	0.05	0.03	0.04	0.03
O (16)	0.02	0.01	0.01	0.01
O (17)	0.05	0.03	0.03	0.03
O (18)	0.05	0.03	0.04	0.03
Ti (19)	0.05	0.03	0.03	0.02

Table 3

Charges on atoms (in ***e***) situated in the defective region containing either the V_0 or F center. The atomic numeration corresponds to the one given in Fig. 5.

ATOM	CUBIC			TETRAGONAL		
	Pure	V_0	F center	Pure	V_0	F center
Sr (1)	1.68	1.70	0.81	1.68	1.71	0.65
O (2)	-1.11	-1.10	-0.99	-1.08	-1.09	-0.97
O (3)	-1.11	-1.05	-0.92	-1.08	-1.02	-0.90
O (4)	-1.11	-1.07	-0.92	-1.08	-1.03	-0.89
Ti (5)	1.80	1.78	1.79	1.73	1.69	1.70
Ti (6)	1.80	1.58	1.59	1.72	1.51	1.61
O (7)	-1.11	-1.09	-1.07	-1.05	-1.05	-1.00
O (8)	-1.02	-1.02	-1.04	-1.01	-1.01	-1.02
O (9)	-1.02	-1.00	-1.05	-0.99	-0.98	-1.01
Sr (10)	1.68	1.64	1.65	1.67	1.65	1.66
O (11)	-1.11	-1.13	-1.11	-1.08	-1.11	-1.08
O (12)	-1.11	-1.20	-1.17	-1.07	-1.19	-1.12
Sr (13)	1.68	1.70	0.85	1.68	1.70	0.75
Sr (14)	1.68	1.65	1.65	1.67	1.65	1.66
O (15)	-1.11	-1.07	-0.99	-1.08	-1.11	-1.08
O (16)	-1.11	-1.05	-1.10	-1.08	-1.05	-1.07
O (17)	-1.11	-1.08	-1.09	-1.08	-1.05	-1.08
O (18)	-1.11	-1.08	-1.10	-1.08	-1.05	-1.09
Ti (19)	1.80	1.78	1.79	1.73	1.69	1.75

Figure captions

Fig. 1. Three-dimensional sketch of the $SrTiO_3$ (110) surface. Black, gray and white balls denote strontiums, titaniums and oxygens, respectively.

Fig. 2. Two-dimensional sketch of the $SrTiO_3$ (110) surface showing negatively and positively charged layers. The arrows show the directions of atomic displacements perpendicular to the surface.

Fig. 3. Density of states (DOS) for the $SrTiO_3$ (110) surface in the cubic phase. The bold line in the upper valence band denoting the Ti 3d states points out the considerable covalence effects in the chemical bonding of the crystal. The 'zero' value of the energy is attributed to the top of the upper valence band.

Fig. 4. DOS for the $SrTiO_3$ (110) surface in the tetragonal phase. The bold line in the upper valence band denoting the Ti 3d states points out even stronger covalence effects compared to the case of the cubic phase of the crystal. The 'zero' value of the energy is attributed to the top of the upper valence band.

Fig. 5. V_0 or F center, shown dashed, on the $SrTiO_3$ (110) surface and its surrounding along the vertical <001> direction. Small, medium and large spheres denote oxygen, titanium and strontium atoms, respectively. The arrows show the directions of atomic movements.

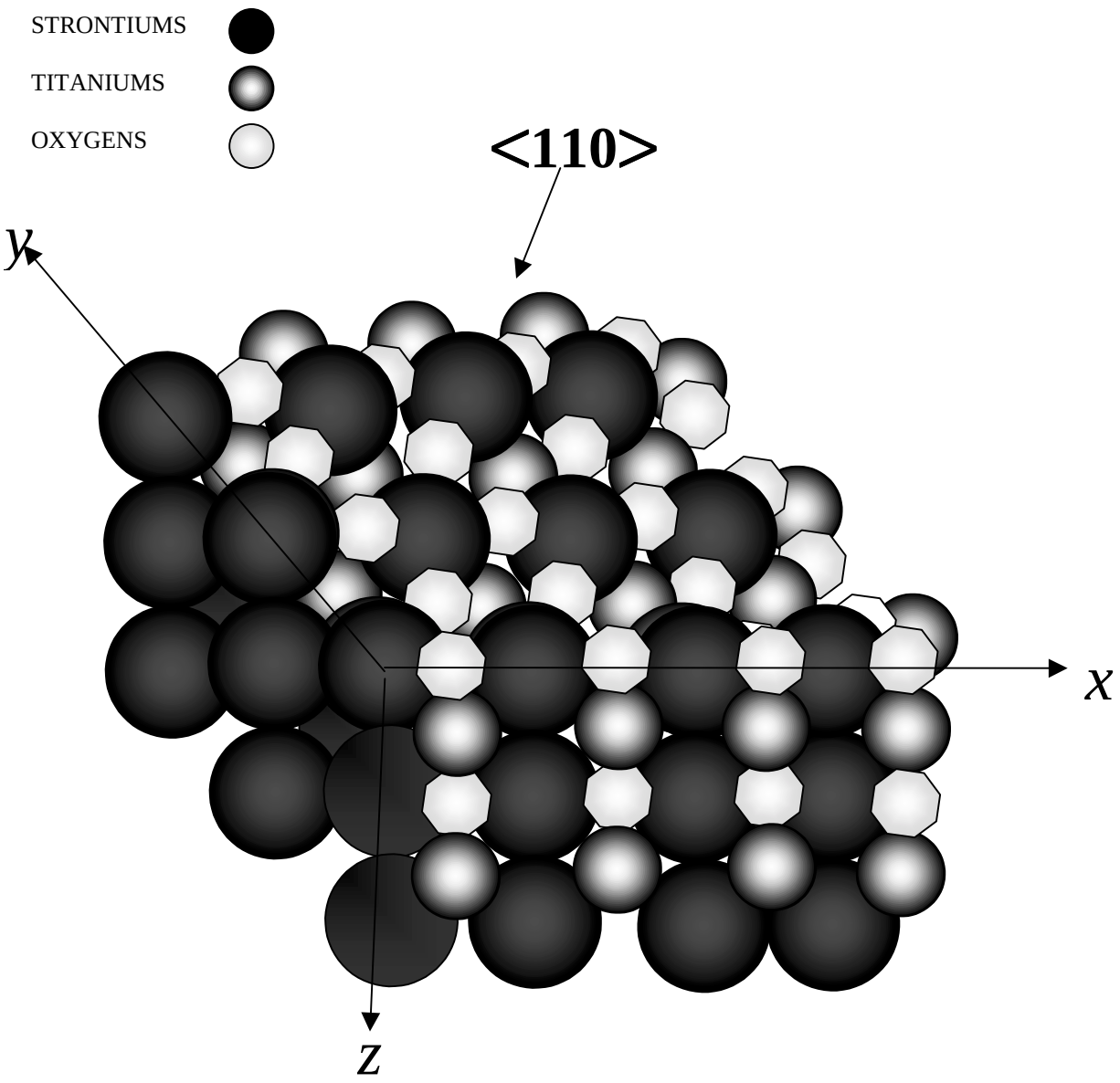
STRONTIUMS
TITANIUMS
OXYGENS
<110>
y
x
z

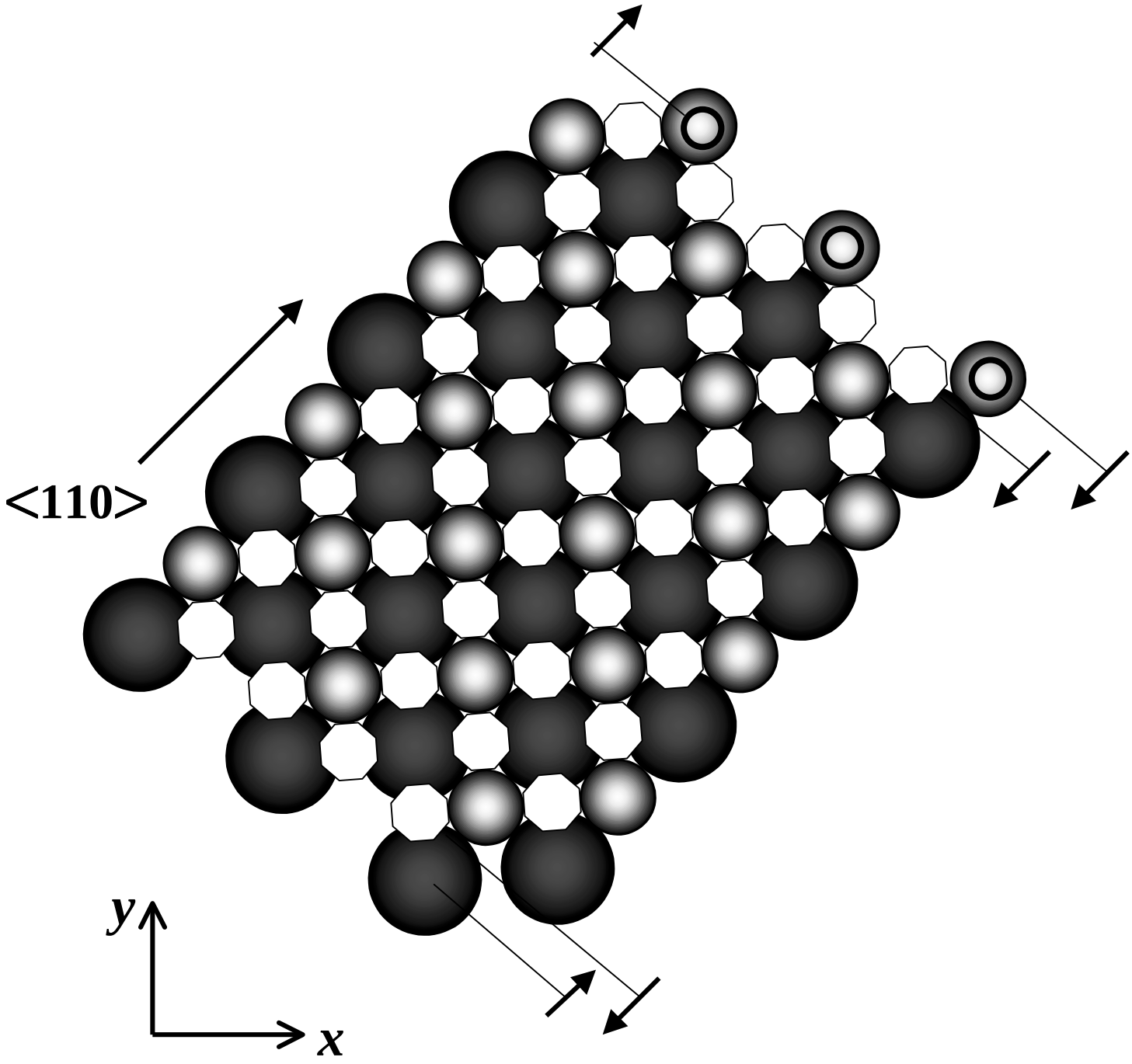
<110>
y
x

Arbitrary Units

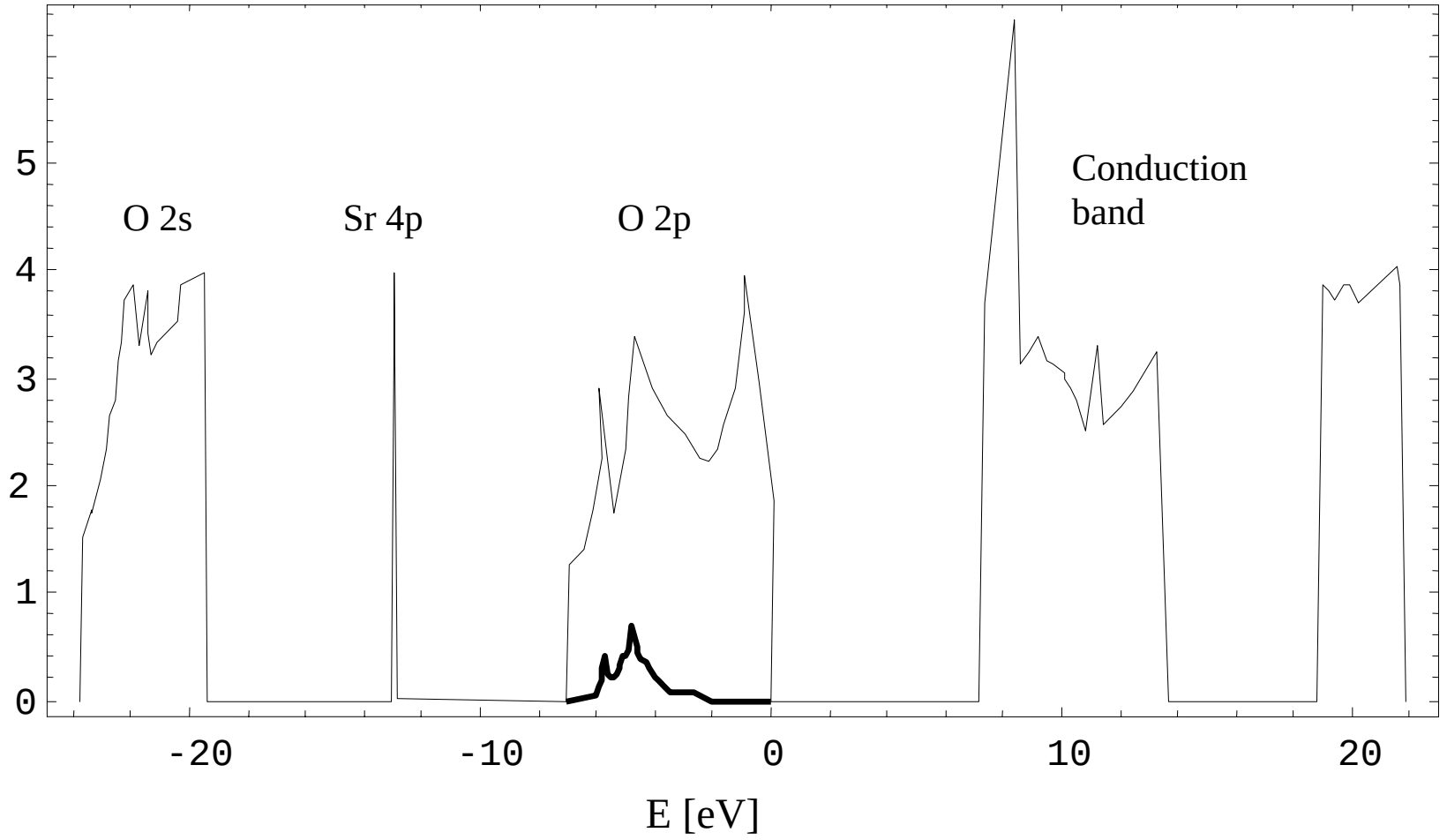

Arbitrary Units

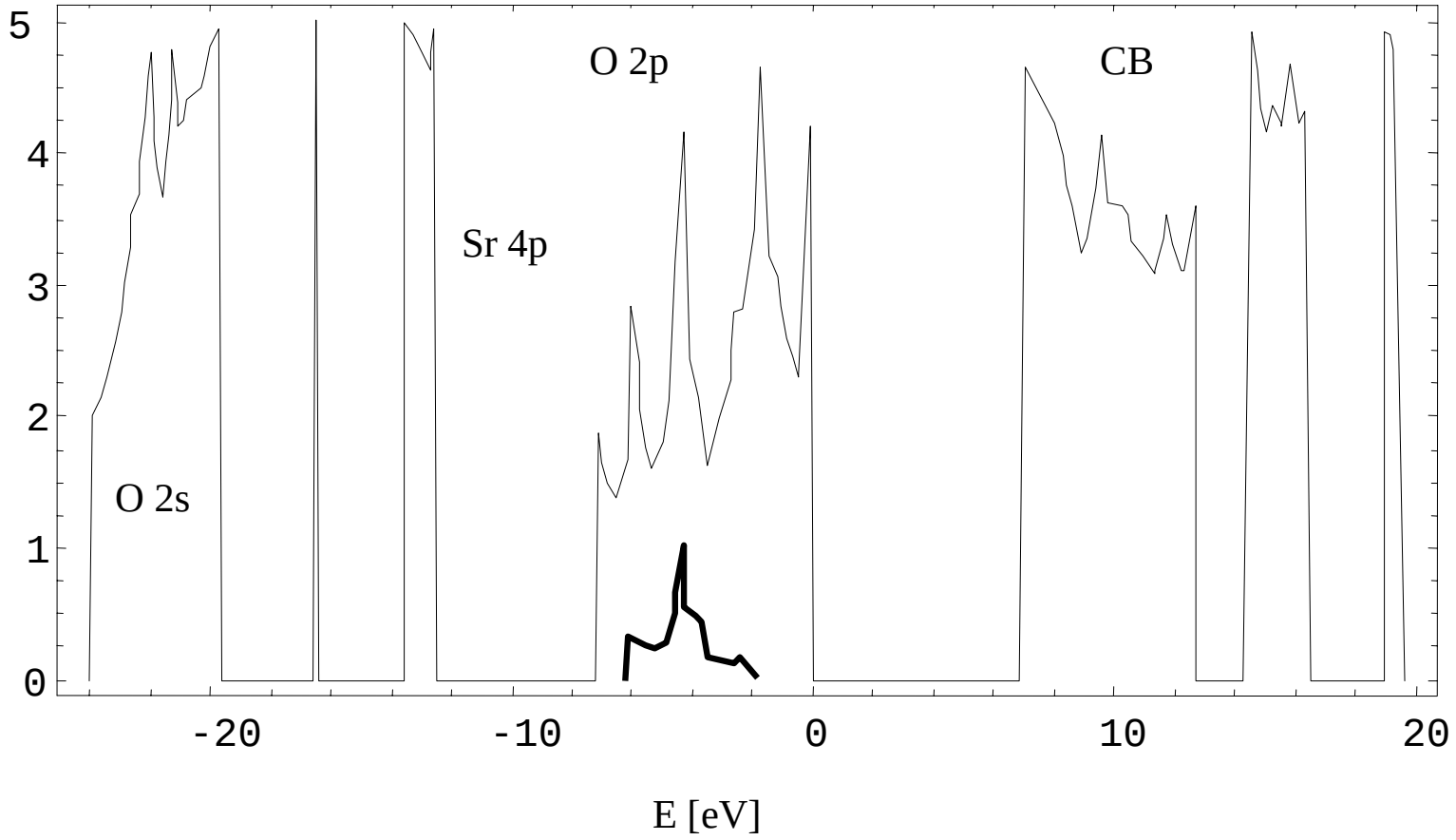

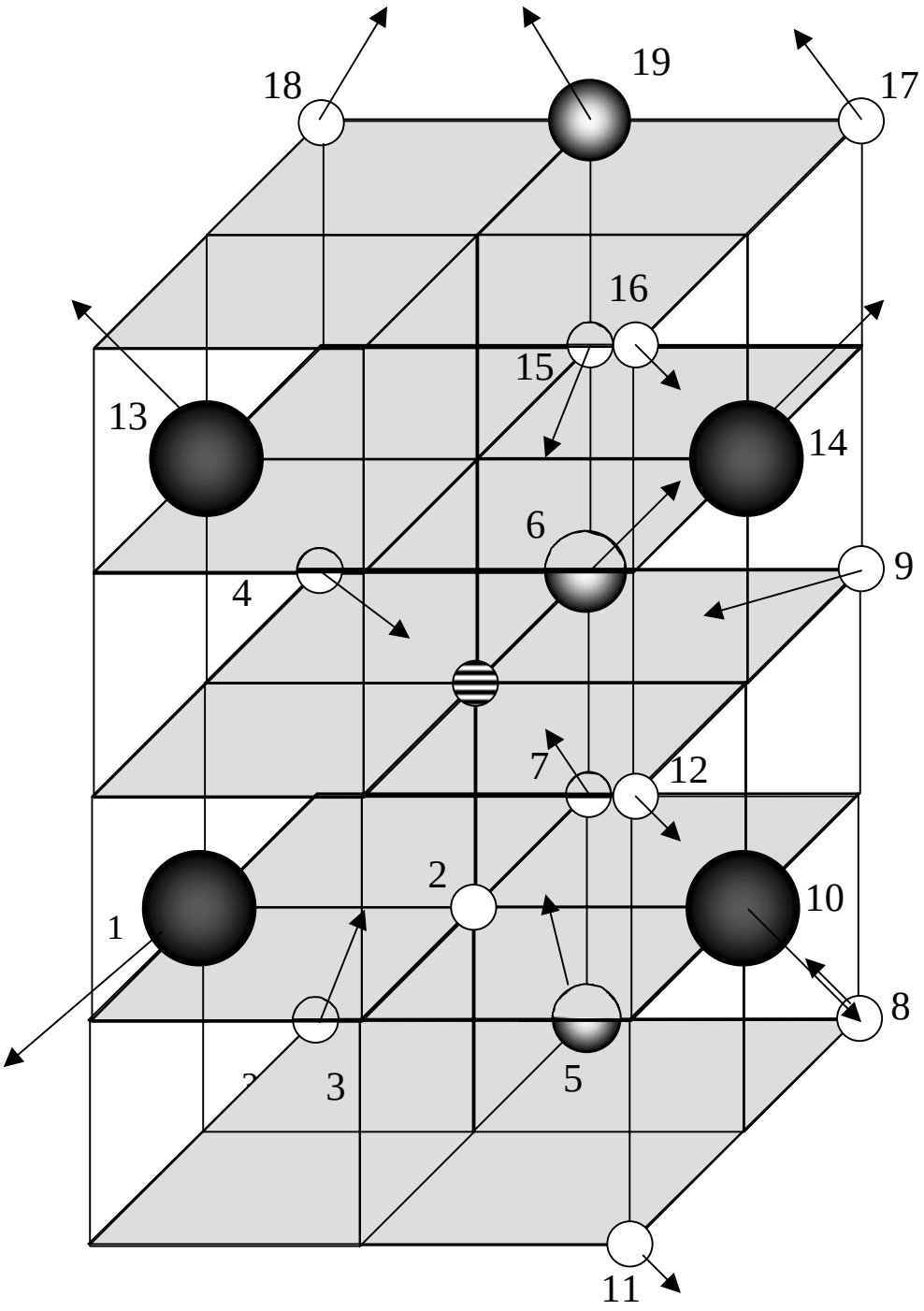
18
19
17
16
15
13
14
6
9
4
7
12
2
10
1
8
3
5
11